

Journal Pre-proofs

Development of an immediate release excipient composition for 3D printing via direct powder extrusion in a hospital

Moritz Rosch, Tobias Gutowski, Michael Baehr, Jan Eggert, Karl Gottfried, Christopher Gundler, Sylvia Nürnberg, Claudia Langebrake, Adrin Dadkhah

PII: S0378-5173(23)00638-5
DOI: <https://doi.org/10.1016/j.ijpharm.2023.123218>
Reference: IJP 123218

To appear in: *International Journal of Pharmaceutics*

Received Date: 19 May 2023
Revised Date: 7 July 2023
Accepted Date: 8 July 2023

Please cite this article as: M. Rosch, T. Gutowski, M. Baehr, J. Eggert, K. Gottfried, C. Gundler, S. Nürnberg, C. Langebrake, A. Dadkhah, Development of an immediate release excipient composition for 3D printing via direct powder extrusion in a hospital, *International Journal of Pharmaceutics* (2023), doi: <https://doi.org/10.1016/j.ijpharm.2023.123218>

This is a PDF file of an article that has undergone enhancements after acceptance, such as the addition of a cover page and metadata, and formatting for readability, but it is not yet the definitive version of record. This version will undergo additional copyediting, typesetting and review before it is published in its final form, but we are providing this version to give early visibility of the article. Please note that, during the production process, errors may be discovered which could affect the content, and all legal disclaimers that apply to the journal pertain.

© 2023 Published by Elsevier B.V.



Development of an immediate release excipient composition for 3D printing via direct powder extrusion in a hospital

Moritz Rosch ^{a,1}, Tobias Gutowski ^{a,1}, Michael Baehr ^a, Jan Eggert ^a, Karl Gottfried ^c, Christopher Gundler ^c, Sylvia Nürnberg ^c, Claudia Langebrake ^{a,b} and Adrin Dadkhah ^{a,b,2}

^a Hospital Pharmacy, University Medical Center Hamburg-Eppendorf, Hamburg, Germany

^b Department of Stem Cell Transplantation, University Medical Center Hamburg-Eppendorf, Hamburg, Germany

^c Institute for Applied Medical Informatics, University Medical Center Hamburg-Eppendorf, Hamburg, Germany

Abstract: 3D printing offers the possibility to prepare personalized tablets on demand, making it an intriguing technology for hospital pharmacies. For the implementation of 3D-printed tablets into the digital Closed Loop Medication Management system, the required tablet formulation and development of the manufacturing process as well as the pharmaceutical validation were conducted. The goal of the formulation development was to enable an optimal printing process and rapid dissolution of the printed tablets for the selected model drugs Levodopa/Carbidopa. The 3D printed tablets were prepared by direct powder extrusion. Printability, thermal properties, disintegration, dissolution, physical properties and storage stability were investigated by employing analytical methods such as HPLC-UV, DSC and TGA. The developed formulation shows a high dose accuracy and an immediate drug release for Levodopa. In addition, the tablets exhibit high crushing strength and very low friability. Unfortunately, Carbidopa did not tolerate the printing process. This is the first study to develop an immediate release excipient composition via direct powder extrusion in a hospital pharmacy setting. The developed process is suitable for the implementation in Closed-Loop Medication Management systems in hospital pharmacies and could therefore contribute to medication safety.

Keywords: 3D Printing; Direct Powder Extrusion; Personalized Medicine; Formulation Development; Closed Loop Medication Management; Immediate Release Tablet

1. Introduction

With further advancements in medicine, the need for individually dosed medications is becoming increasingly apparent. Additive manufacturing (AM), which is often referred to as 3D printing (3DP), is a computer-controlled process that comprises several different technologies. Some of these offer the possibility to be used in the manufacturing of pharmaceuticals, for example, binder jetting, fused deposition modeling (FDM), direct powder extrusion (DPE) and semi solid extrusion (SSE).

Current pharmaceutical literature on material extrusion techniques is focused on FDM (Chamberlain et al., 2022; Goyanes et al., 2015a; Hoffmann et al., 2022; Kissi et al., 2021; Krueger et al., 2023; Windolf et al., 2021) and SSE (Díaz-Torres et al., 2023; Liang et al., 2023; Rodríguez-Pombo et al., 2022; Seoane-Viaño et al., 2021a; Tagami et al., 2021; Yan et al., 2020; Yu and Chen, 2020; Zhu et al., 2022). Both technologies are readily available and offer the possibility of producing relatively small batches, which limits the amounts of active pharmaceutical ingredient (API) and excipients needed to conduct formulation studies.

In addition to the printer, FDM requires a hot melt extruder to manufacture the drug-loaded filament that serves as a feedstock in the printing process. This not only limits the selection of excipients, as the filaments need to match specific mechanical properties in order to be usable as feedstock, but also increases thermal stress on the API. As an alternative, SSE enables the use of pre-filled syringes from which a gel or paste is extruded but often requires a post-printing solidification process.

Abbreviations: 3DP, 3D printing; AM, additive manufacturing; API, active pharmaceutical ingredient; BZ, Benserazide; CAD, computer-aided design; CD, Carbidopa; CLMM, closed-loop medication management; CMA, critical material attribute; CPP, critical process parameter; CQA, critical quality attribute; DPE, direct powder extrusion; DSC, differential scanning calorimetry; FDM, fused deposition modelling; HPLC, high-performance liquid chromatography; LD, Levodopa; PAT, process analytical technology; SD, standard deviation; SSE, semi solid extrusion; T_g, glass transition temperature; TGA, thermogravimetric analysis; T_m, melting temperature; UDB; unit dose bag

¹ First Authors

² Corresponding author: at Martinstraße 52, 20246 Hamburg, E-Mail address: a.dadkhah@uke.de

In contrast, DPE can be viewed as a single-step process in which the powder blend is directly added to the printhead, fed towards the heated nozzle by a single screw and subsequently extruded in order to print the designed object in a layer-by-layer fashion (Goyanes et al., 2019). It has been reported that the powder flow exhibits a considerable influence on the printing process in DPE (Boniatti et al., 2021). This could pose a challenge for the implementation in hospital pharmacies as it limits the formulation options. Hospital pharmacies are often not equipped to granulate powders quickly and efficiently and are therefore dependent on commercially available product qualities or additives to increase powder flow. Other than that, DPE poses a viable option for the manufacturing of extemporaneous formulations in hospital pharmacies, since there is no need for a complex and time consuming, preceding feedstock preparation or post-printing process. Moreover, the printer can be used with only a few grams of the powder blend, which allows a more cost-efficient formulation development and enables the manufacturing of very small batch sizes in clinical practice. However, using DPE to manufacture solid oral dosage forms in a clinical setting has not been established yet.

In general, AM is an intriguing technology for the implementation in hospital pharmacies. At times, the medication for specific therapeutic approaches or patient groups is not commercially available and therefore needs to be manufactured by (hospital) pharmacies. Most commonly, if there is the need for individually dosed solid oral dosage forms, capsules are prepared. To achieve an adequate level of content uniformity, large numbers of capsules with a fixed dose need to be prepared, which makes frequent dose changes based on the measurement of drug levels, biomarkers or current symptom control challenging. In contrast, AM facilitates the manufacturing of individually dosed solid oral dosage forms since it offers the possibility of printing different doses on demand with a high level of precision and accuracy of the doses (Seoane-Viaño et al., 2021b; Vaz and Kumar, 2021).

Furthermore, the digital nature of 3DP makes the integration of manufacturing personalized medicines into an existing digital medication process in hospitals, such as the closed-loop medication management (CLMM) (Baehr and Melzer, 2018), feasible and might therefore contribute to improving medication safety for inpatients (Berger et al., 2022). However, there are no findings regarding the integration of compounding personalized solid oral dosages by AM into a digital medication process in a clinical setting.

Due to a shift towards precision dosing for numerous indications (Vinks et al., 2019) coupled with recent advancements in digital health monitoring systems (Bayoumy et al., 2021; Bruno et al., 2020; Kim et al., 2020; Pahwa et al., 2020; Powers et al., 2021), the benefits of personalized pharmacotherapy are becoming increasingly apparent. For instance, patients with Parkinson's disease often require more than four doses of Levodopa (LD) / Carbidopa monohydrate (CD) per day in different dosages (Fox et al., 2018) that are often compiled from fragmented, marketed drug products (Forough et al., 2018). However, due to the symptoms (e.g., tremor and dysphagia) of the disease, patients often have problems handling and swallowing (Buhmann et al., 2019) tablets and therefore may benefit from the flexibility of AM to print individual doses and tablet geometries on demand. This might reduce the potential of medication errors, as it eliminates the need to compile the intended dose with fragmented tablets, which poses a two-fold risk. First, the wrong tablet might be split or some fragments could be lost due to disease-related motor symptoms of the patient. Secondly, it has been shown that quarters of tablets with a score-line are often not dose equivalent and the standard deviation (SD) of the dose is relatively high (up to 19.3%) (Madathilethu et al., 2018), whereas in comparison, DPE often reaches SDs below 5% (Ong et al., 2020; Pflieger et al., 2022). In addition, the therapy of Parkinson's disease with LD / CD often requires an immediate drug release to achieve adequate symptom control. However, there is no data on a rapidly disintegrating DPE formulation without an elaborate feedstock preparation, of doses up to 200 mg, which is integral for the intended use of the tablets.

Therefore, this study aimed to demonstrate the feasibility of developing an excipient composition that enables an immediate drug release and reliable printing properties within DPE, in a hospital setting. Additionally, the resulting tablets should exhibit high hardness values and a storage stability sufficient for our CLMM. For that purpose, LD and CD were identified as model APIs of high clinical interest (Langebrake et al., 2023). The study presented here is a part of a larger project that comprises the tablet formulation, manufacturing process development and analytics as well as the development of a digital infrastructure and a machine learning based decision-support-system, which will be published separately.

2. Materials and Methods

2.1. Materials

LD and CD were gifted by Desitin Arzneimittel GmbH (Hamburg, Germany). Benserazide-HCl (BZ) was gifted by Deva Holding A.S. (Istanbul, Turkey). Mass values [mg] and dosages of tablets always refer to Carbidopa and Benserazide base, respectively. Kollidon® VA 64 (vinylpyrrolidone-vinyl acetate copolymer) and Kollicoat® IR (polyvinylalcohol-polyethylene glycol graft copolymer) were gifted by BASF SE (Ludwigshafen, Germany). Mannogem® XL Ruby (mannitol) and Compressol® SM (co-processed Sorbitol and Mannitol) were donated by SPI Pharma (Wilmington, NC, USA) via Lehmann&Voss&Co. KG (Hamburg, Germany). Sodium dihydrogen phosphate dihydrate (NaH_2PO_4 , Emsure®), di-Sodium hydrogen phosphate dihydrate (Na_2HPO_4 , Emsure®), phosphoric acid (H_3PO_4 , LiChropur™), hydrochloric acid (HCl, Titripur®) and water for HPLC analysis were purchased from Merck KGaA (Darmstadt, Germany). Methanol in gradient grade (Chemsolute®) was purchased from Th. Geyer GmbH & Co. KG (Renningen, Germany). FDS/Proud packaging material consisting of multiple layers (Polyethylene and Cellophane 300, 20 μm thickness each; Baxter code: P1601 [P2010]) was manufactured by Yuyuma Co, Ltd (Osaka, Japan). Brown glass packaging was purchased from Zscheile & Klinger GmbH (Hamburg, Germany).

2.2. Methods

2.2.1. Blending of powders

For each batch, 50 – 100 g of a blend of APIs and the excipients were weighed and blended with a FagronLab™ InvoMatic blender (Fagron GmbH & Co. KG, Glinde, Germany) at 50 rpm for 10 min. Table 1 shows the formulations that were evaluated.

2.2.2. Flowability

Flowability of batch P25/29-M was determined in triplicate following Ph. Eur. 10.6/2.9.16 (EDQM, 2021) on a PTG S3 powder analyzer (Pharma Test Apparatebau AG, Hainburg, Germany) using nozzle 1.

2.2.3. Angle of repose

Three measurements of the drained angle of repose method according to Ph. Eur. 10.6/2.9.36 (EDQM, 2021) were conducted with batch P25/29-M on a PTG S3 powder analyzer (Pharma Test Apparatebau AG, Hainburg, Germany).

2.2.4. Bulk density and tapped density of powders

Bulk and tapped densities of batch P25/29-M were measured using method 1 as described in Ph. Eur. 10.6/2.9.34 (EDQM, 2021). Tapped density was measured with an Engelsmann jolting volumeter type EU42E2/114S-WF (J. Engelsmann AG, Ludwigshafen, Germany). The measurements were performed three times. Hausner factor and Carr's index were calculated as suggested (Carr, 1965).

2.2.5. Particle size analysis by laser light diffraction

Laser diffraction measurements were performed with an LS 13 320 laser diffraction particle size analyzer equipped with a Tornado DPS module (Beckman Coulter Inc, Brea, CA, USA). Each API, excipient and the blend of batch P25/29-M were measured five times. Particle sizes were calculated using the Fraunhofer method as suggested in Ph. Eur. 10.6/2.9.31 (EDQM, 2021)

2.2.6. Differential scanning calorimetry (DSC)

DSC analyses were carried out with a DSC 1 device (Mettler-Toledo, LLC, Columbus, OH, USA) operated with STARe Software V16.10. Every single component of the formulation as well as the powder blend and the extruded filament (both P25/29-M) were analyzed. Three different methods were utilized. Nitrogen was used as a purging gas at a flow rate of 50 mL/min. Every sample was heated to 250 °C (10 °C/min) and kept at this temperature for 5 min. CD, LD, mannitol and the powder blend were also heated (10 °C/min) to and kept at 185 °C (10 min), then cooled to 25 °C (20 °C/min) and kept at this temperature for 5 min and reheated to 185 °C (10 °C/min) and kept at this temperature for 10 min. Ultimately, CD and the powder blend were also heated to 182 °C (10 °C/min) and kept at this temperature for 30 min.

2.2.7. Thermogravimetric analysis (TGA)

TGA analyses were carried out with a Discovery TGA (TA Instruments, Waters, LLC, U.S.A.) and data was collected and analyzed with TA Instruments Trios software and percent mass loss or onset temperature were calculated. Two different methods were utilized. Both APIs were subjected to a temperature ramp of 10 °C/min starting at 40 °C and concluding at 300 °C in open aluminum pans. CD was additionally subjected to an isothermal stress test at 180 °C for 30 min.

2.2.8. 3D printing of tablets (DPE)

The previously blended powders were 3D printed using a M3DIMAKER™ equipped with a DPE printhead coupled with a 0.4 mm nozzle (FabRx Ltd., London, United Kingdom). Computer-aided design (CAD) models of tablets were designed using Autodesk Tinkercad (Autodesk Inc., Mill Valley, CA, U.S.A.) and processed with Repetier-Host software (Hot-World GmbH & Co. KG, Willich, Germany). To enhance powder flow, the M3DIMAKER™ was modified with a custom-made stirrer (Figure 3).

Tablets were printed using the following parameters: printing temperature: 180 °C; first layer height: 0.6 mm, layer height: 0.15-0.30 mm (adaptive slicing), infill: 60-100%, travel speed 70 mm/s, first layer speed 5 mm/s, perimeter speed 7.5-15 mm/s, infill speed: 15-20 mm/s with zero (Oblongs) or one (Cylinders and Donuts) top layer, two bottom layers and two shells.

The following dose range was identified as clinically desirable: 60-170/15-42.5 mg LD/CD. Each of the three shapes was printed in a small (60/15 mg) and large (170/42.5 mg) model. The CAD models had the following measures for the different dosages and formulations: small Donut: diameter 10.5 mm, height: 2.71-2.89 mm, inner hole diameter: 4 mm; large Donut: diameter: 12 mm, height: 5.75 mm, inner hole diameter: 4 mm; small Cylinder: diameter 10.5 mm, height: 2.71 mm; large Cylinder: diameter 12 mm, height: 5.5-5.89 mm; small Oblong w/ reduced infill: 14x7x3.1 mm; large Oblong w/ reduced infill: 21x8.5x 5 mm.

2.2.9. Friability of uncoated tablets

Friability of the printed Donuts of batch P25/29-M was measured according to Ph. Eur. 10.6; 2.9.7 (EDQM, 2021), using an AE-2 friability tester (Biomation GmbH, Jugenheim, Germany). 100 rotations were performed at 25 rpm. Afterwards, the tablets were dedusted, weighed and the loss of mass [%] was determined.

2.2.10. Resistance to crushing

The measurements were performed according to Ph. Eur. 10.6; 2.9.8 (EDQM, 2021), using an Erweka TBH 525 TD hardness tester (Erweka GmbH, Langen, Germany). The Oblongs were aligned so that the force was applied longitudinally. If a measurement exceeded the maximum force of the device (500 N), a crushing strength of 500 N was assumed for calculations and comparisons. Ten measurements were recorded per batch.

2.2.11. Tensile strength

Tablet size measurements were conducted using a Digital ABS AOS Caliper (Mitutoyo Corporation, Kawasaki, Japan). Together with the previously described crushing strength values (2.2.10.) tensile strength (σ) of the printed tablets was calculated for the Cylinders (Equation 1) as described by Fell et al. (Fell and Newton, 1968):

$$\sigma = \frac{2P}{\pi DT} \quad (1)$$

P = crushing strength [N]; D = tablet diameter [mm]; T = tablet thickness [mm]

For the calculation of the Donut's tensile strength, it was decided to subtract the diameter of the inner hole of the tablets from D in order to ensure a meaningful comparison. The Oblongs were calculated using their width as D.

2.2.12. Disintegration

Disintegration analyses were conducted based on Ph. Eur. 10.6; 2.9.1 (EDQM, 2021), with a ZT41 disintegration tester (Erweka GmbH, Langen, Germany). In order to keep consistent analytical conditions, the same medium (0.1 M HCl) as for dissolution experiments was used. Discs were used for disintegration testing. For each constitution and shape, two tablet sizes were analyzed respectively. The investigated tablet sizes represent the upper and lower end of the selected dose range.

To simplify the comparison of the different formulation's shapes and sizes, the average disintegration rate (Equation 2) was calculated.

$$\text{Average disintegration rate} \left[\frac{mg}{s} \right] = \frac{\text{Tablet mass [mg]}}{\text{Disintegration time [s]}} \quad (2)$$

2.2.13. Dissolution & Content analysis

Dissolution experiments were carried out according to Ph. Eur. 10.6; 2.9.3 (EDQM, 2021) with a Premiere 5100 Dissolution System (Distek Inc., North Brunswick Township, NJ, USA). 900 mL of 0.1 M HCl was used as dissolution medium as suggested in Ph. Eur. 10.6; 5.17.1 (EDQM, 2021). Three different shapes of P25/29-M were evaluated. For each shape, six tablets were analyzed in parallel. The paddle speed was set to 100 rpm. Samples were taken after 5, 10, 15, 20, 30, 45, 60 and 90 min. A sinker was used for analyses. For all small tablets and the large Oblongs a Distek "Japanese Basket" was used, whereas a custom 3D printed polylactic acid (PLA) sinker (Figure 1) was used for the large Cylinders and the large Donuts. If applicable, the dissolution profiles were compared using the f2 comparison (Moore and Flanner, 1996).

The API content of the powder blend and the dissolution samples were analyzed and evaluated with a Nexera XR HPLC system and LabSolutions software version 6.83 (both Shimadzu Corp., Nakagyo-ku, Kyōto, Japan). The Nexera XR HPLC system consists of two degassing units (DGU-20A5R) and two HPLC-pumps (LC-20ADXR) as well as an autosampler (SIL-20ACXR), a column oven (FCV-34AH), an UV-Detector (SPD-M20A 230V) and a communication bus module (CBM-20A).

Samples were dissolved and diluted in 0.1 M HCl. Turbid samples were filtered through a 0.22 μm PTFE Filter. Prior to each analytical sequence, the column was equilibrated for 30 min and the autosampler was purged for 5 min. HPLC samples were measured in duplicate with an injection volume of 20 μL. An endcapped RP-18 column (LiChrospher® 100 RP-18 endcapped (5 μm), LiChroCART® 250-4.6 HPLC Cartridge) coupled with an RP-18 guard column (LiChrospher® 100 RP-18 (5 μm), LiChroCART® 4-4 Guard Column) (both Merck KGaA, Darmstadt, Germany) was utilized during analysis. The column oven was set to 35 °C and the total flow rate was set to 1.25 mL/min. The mobile phase was a 90:10 mixture of a hydrogen phosphate buffer (20 mM NaH₂PO₄ + 10 mM Na₂HPO₄ at pH 4) and methanol. Both APIs were detected at a wavelength of 280 nm and showed retention times of 2.94 min (LD) and 4.30 min (CD). An external, six-level calibration was used. LD was calibrated in the range of 25–250 μg/mL, whereas CD was calibrated in the range of 6.25–62.5 μg/mL. This method was modified on the basis of the method presented by Raut and Charde (Raut and Charde, 2014) and validated according to ICH Guideline Q2(R2) (ICH, 2022).

For LD and BZ analytics, a separate HPLC method was developed for the same equipment. The mobile phase was a 95:5 mixture of the aforementioned hydrogen phosphate buffer (pH 2.5) and methanol. LD was detected at 280 nm and BZ at 268 nm. Retention times were 3.41 min (BZ) and 4.41 min (LD). The calibration for LD was the same as in the above-named method and BZ was calibrated in the same range as CD. This method was developed in the hospital pharmacy and validated according to ICH Guideline Q2(R2) (ICH, 2022).

2.2.14. Stability analysis

Small Donuts of P25/29-M were packed in FDS/Proud packaging material Unit Dose Bags (UDB) using an FDS II Proud 336 device (Baxter International Inc., Deerfield, IL, USA) or brown glass stored in constant climate chambers (KBF P 240 and KBF S 240; Binder GmbH; Tuttlingen, Germany). The constant climate chambers were set to 25 °C / 60% RH and 40 °C / 75% RH as suggested for long-term and accelerated stability testing (ICH, 2003). Samples packed in UDB were stored for 7 days or 28 days in each of the previously mentioned conditions. Samples in brown glass were stored for 28 days in the 25 °C / 60% RH condition. After storage, the API contents of the samples were analyzed via HPLC as described in 2.2.6. Each sampling time comprised three samples.

2.2.15. Statistical analysis

IBM SPSS statistics Version 27.0.1.0 (IBM Corporation; Armonk, NY, USA) was used for statistical calculations. Results were compared with ANOVA. Significance was assumed for p-values < 0.05.

3. Results

It was possible to develop an immediate release excipient composition for DPE-based 3DP, which allows printing of different shapes (Figure 1: 3D printed PLA sinker, scale in cm

Figure 2), in a hospital setting. The following subsections present detailed results regarding the pre-manufacturing screening of the excipients and the powder blend. Moreover, the manufacturing process as well as the thorough characterization of the resulting tablets are illustrated.

3.1. Powder screening

In order to ensure a constant feed rate, the flowability of the powder formulation is of high importance. Flowability has been reported to be a considerable challenge in DPE (Boniatti et al., 2021). The formulation P25/29-M showed passable powder flow characteristics according to Carr's Classification ($20.92\% \pm 1.08\%$), angle of repose ($41.1^\circ \pm 0.12^\circ$) and Hausner factor (1.26 ± 0.02) (Carr, 1965). The values were calculated from bulk (0.46 g/mL) and tapped densities (0.58 g/mL). The powder flow hung up during the measurements and had to be mechanically induced. Consequently, the flow time could not be measured. Median particle sizes of $d_{50} = 15.3 \text{ }\mu\text{m}$ (CD) up to $d_{50} = 345 \text{ }\mu\text{m}$ (mannitol) were measured, while the blend P25/29-M showed the following values: $d_{10} = 19.2 \text{ }\mu\text{m}$, $d_{50} = 96.1 \text{ }\mu\text{m}$, $d_{90} = 258 \text{ }\mu\text{m}$. During printing, core flow behavior of the powder resulted in insufficient and inconstant feeding of the DPE printhead by the screw. To eliminate this problem, the utilized DPE printhead was structurally modified. For this purpose, a wire was bent into the shape of an open noose and fitted to the coupling element of the printhead. The wire functions as a force feeder (Figure 3) by constantly moving the powder bed and thereby ensuring that the screw transports the powder blend to the heating zone and, subsequently, the nozzle of the DPE printhead. Through this modification, a constant powder feed rate was achieved, which was necessary to print tablets with uniform weight and API content.

3.2. Thermal screening

As DPE is based on melt extrusion and, thereby, a thermally stressing process, it is essential to investigate which temperatures the APIs of interest tolerate. This, in turn, helps with the choice of suitable excipients and enables the selection of the printing parameters.

Literature states that LD has a melting temperature (T_m) of $284\text{-}285^\circ\text{C}$ (Ledeti et al., 2018) and CD melts at 207°C (Ajit et al., 2018). Additionally, some sources state that CD decomposes at the T_m . To confirm literature data, DSC (Figure 4) and TGA (Figure 5) experiments were carried out.

The DSC diagram of LD shows a glass transition at 179.6°C followed by a molecular relaxation. As expected, no melting peak was found, as the analysis was stopped 34°C below the literature melting point of 284°C . The DSC diagram of CD shows a large endothermic event spanning from ca. 100°C to about 165°C and a second event slightly above 200°C , which is, as described in the literature, followed by a decomposition. The thermogram of LD has no mass loss until about 275°C , whereas the thermogram of CD shows a mass loss of about 8% between ca. $90\text{-}140^\circ\text{C}$.

Based on the API data, the excipients were chosen. The excipients, as well as the powder blend (P25/29-M) and the resulting filament were subjected to the same DSC (Figure 6) method as the APIs. According to literature, Kollicoat® IR has a glass transition temperature (T_g) of 45°C and a T_m of 208°C (Kolter et al., 2012). DSC showed a glass transition at about 48°C and an endothermic event with an onset at 203°C . Literature states that Kollidon® VA64 has a T_g of 101°C (Kolter et al., 2012). The DSC diagram shows a glass transition at about 100°C . Mannitol is a well-characterized substance with a T_m of $165\text{-}170^\circ\text{C}$ (Jüptner, 2022). DSC analysis revealed a sizeable endothermic event with an onset of 165.9°C .

After dissolution experiments CD (DSC and TGA) and the powder blend (DSC) were subjected to alternative thermoanalytical methods, which exposed the samples to an increased temperature (isothermal) for a prolonged time. The DSC diagram of CD (Figure 7) shows that after an exposition to 182°C for 7-

8 min, CD begins to decompose, whereas no events can be found in the diagram of the powder blend (Figure 7). The thermogram of CD (Figure 8) shows a loss in mass of more than 20% over the first 10 min, followed by a decelerated mass loss until the end of the analysis.

3.3. Manufacturing process and formulation screening

Printability was considered reliable, when continuous polymer melt extrusion, an adequate build plate and between-layer adhesion as well as a high uniformity of tablet weight were achieved. Moreover, an appreciable hardness as well as an immediate release profile and a precise API content were the most Critical Quality Attributes (CQAs) of the Quality Target Product Profile (QTTP) of this tablet that was intended for clinical use (ICH, 2009; Yu et al., 2014). Printing temperature, feed rate and infill pattern were identified as the most Critical Process Parameters (CPPs). Solubility of the formulation, decomposition temperature of the APIs and excipients as well as flowability of the powder blend were identified as the most Critical Material Attributes (CMAs).

The constitution of the formulation was constantly optimized. The percentage of the BCS class I APIs was gradually increased from 25-35.56%. Kollidon® VA 64 and Kollicoat® IR were selected as polymer components providing adequate water solubility. Mannitol, Compressol® SM or citric acid monohydrate were added as a plasticizer.

Initially, the plasticizers were optimized (Table 1). Afterwards, the polymer ratios were evaluated for their influence on the disintegration speed of the formulation and its build plate adhesion before, finally, the impact of three different shapes (Cylinder, Donut, Oblong) on the disintegration and later dissolution behavior was investigated.

Experiments with the three plasticizers showed that Mannitol- and Compressol® SM-containing formulations were printable, while the citric acid-based formulations could not be extruded. P25/29-M was used to evaluate the influence of the different shapes.

The Cylinder was used as the initial shape in printing experiments. Afterwards, the Donut with a higher SA/V ratio (surface area to volume) was introduced (Goyanes et al., 2015b; Windolf et al., 2021). Ultimately, it was considered promising to experiment with the infill. The reduction of the infill results in a drastically increased SA/V at the cost of the tablets being considerably larger. Rather than increasing the diameter of the Cylinder, it was chosen to increase the area by introducing the oblong shape, as this shape is somewhat capsule-like and should therefore be easier to swallow than a large cylindrical tablet (Buhmann et al., 2019).

Prior to DPE printing, the API contents of the powder blend P25/29-M were analyzed via HPLC, which confirmed the uniformity of the blend (see chapter 3.6.).

3.4. Hardness

The tested tablets (all P25/29-M) showed average crushing strength values (Table 2) ranging from $62.0 \text{ N} \pm 18.3 \text{ N}$ for the small Donuts up to $465.5 \text{ N} \pm 58.3 \text{ N}$ for the large Cylinders. The true average value of the Cylinders might be considerably higher, since seven of the ten samples were not crushed by the maximum force of the measuring apparatus of 500 N. Therefore, 500 N was used as a value for the samples to calculate the results. Nevertheless, the large Cylinders showed significantly ($p < 0.001$) higher values than each other batch. The small Cylinders also showed significantly higher crushing strengths than all Donuts and Oblongs. The crushing strengths of the large Donuts were significantly higher than those of the small Oblongs and the small Donuts. The large Oblongs show significantly higher values than the small donuts, while the small Oblongs show no significant differences to the two previous batches.

Tensile strength with partly modified calculations (section 2.2.11.) favored the cylindrical tablets as well (small: $5.48 \text{ N/mm}^2 \pm 1.67 \text{ N/mm}^2$; large: $4.85 \text{ N/mm}^2 \pm 0.65 \text{ N/mm}^2$). Again, the value for the large Cylinders was restricted by the measurement device and would normally be even higher. Tensile strength for the small Oblongs was $3.10 \text{ N/mm}^2 \pm 0.31 \text{ N/mm}^2$ and, therefore, significantly higher than the large Oblongs at $1.85 \text{ N/mm}^2 \pm 0.47 \text{ N/mm}^2$, which show the lowest values. Both Donut formulations (small: $2.18 \text{ N/mm}^2 \pm 0.64 \text{ N/mm}^2$; large: $2.26 \text{ N/mm}^2 \pm 0.27 \text{ N/mm}^2$) show no significant differences to either of the Oblongs.

Tablets of both tested Donut batches showed very low friability. The small Donuts showed 0.025%, while the large Donuts showed an even lower value of 0.017%.

3.5. Disintegration

Disintegration times and rates (

Table 3) of every printable formulation were evaluated.

Statistical evaluation of the disintegration time shows four significantly different groups. The first group consists of the two Oblongs (11-13 min); the second group spans the small Cylinders and small Donuts as well as the large Donuts (21-30 min); the third group is the large Cylinders of powder blend P20/34-M (~43 min) and the final group consists of the remaining large Cylinders (53-54 min).

Comparing the disintegration rates, three formulations stick out: the large Oblongs showed a significantly higher disintegration rate ($p < 0.001$) than every other formulation. Additionally, the large Donuts as well as the small Oblongs, which were statistically similar, stand out. The large Cylinders of P20/34-M were also similar to the small Oblongs but showed a significantly lower disintegration rate than the large Donuts. The remaining formulations were largely comparable.

3.6. Dissolution & Content analysis

Dissolution times and content of all shapes of P25/29-M were evaluated. Each shape was investigated in a larger (LD/CD: 170 mg/42.5 mg) and smaller (LD/CD: 60 mg/15 mg) dose. Every tablet dissolved completely during the experiments. Additionally, the powder blend was analyzed for its API content.

Content analysis of the powder blend showed recoveries of $104.47\% \pm 0.43\%$ (LD) and $100.53\% \pm 0.3\%$ (CD). For the tablets, LD recoveries of $103.2 \pm 4.3\%$ (small) and $100.1 \pm 1.2\%$ (large) for the Cylinders, $104.7 \pm 2.8\%$ (small) and $102.1 \pm 2.4\%$ (large) for the Donuts and $102.6 \pm 3.4\%$ (small) and $102.5 \pm 1.7\%$ (large) for the Oblongs were found. Whereas only $69.4 \pm 10.8\%$ (small) and $66.2 \pm 2.3\%$ (large) from the Cylinders, $64.9 \pm 1.5\%$ (small) and $59.5 \pm 3.2\%$ (large) from the Donuts and $66.7 \pm 6.5\%$ (small) and $62.6 \pm 1.4\%$ (large) from the Oblongs of the theoretical CD content could be recovered.

The dissolution diagram of LD (Figure 9) shows that the six shapes can be classified into two groups. The three small shapes as well as the large Oblongs exhibit a very rapid dissolution. The small Donuts (10 min: $88.01\% \pm 10.73\%$) and Oblongs (10 min: $87.53\% \pm 12.63\%$) as well as the large Oblongs (10 min: $85.44\% \pm 13.49\%$) release more than 80% of their LD in less than 10 min, whereas the small Cylinders (10 min: $78.80\% \pm 8.47\%$; 15 min: $98.20\% \pm 5.52\%$) release 80% slightly slower. The large Cylinders (45 min: $85.68\% \pm 5.76\%$) and Donuts (45 min: $97.82\% \pm 5.83\%$) reach that threshold between 30 min and 45 min. In each case, about 100% of the theoretical LD dose was recovered. The f_2 comparison of the large cylinders and large donuts results in a value of 55.30. Due to the low recovery of CD from the printed tablets the dissolution behavior has to be evaluated carefully. The diagram of CD (Figure 10) shows final concentrations of about 60 – 70%. However, the dissolution behavior regarding the CD seems comparable to that of LD.

Following the dissolution experiments and the subsequently adapted thermoanalyses to further investigate the thermolability of CD, extrusion experiments with BZ were conducted. For these experiments, the CD (P25/29-M) was substituted with BZ. The formulation was extruded between 125-155 °C and the extrudate was analyzed via HPLC. BZ recoveries were 29.52% (125 °C) to 24.61% (155 °C) compared to the powder blend.

3.7. Stability analysis

Stability experiments were conducted to evaluate the formulations stability in its designated primary packaging. After storage in constant climate chambers, the API contents were determined:

Compared to the results of the small Donuts in the previous section that were tested without storage, only the 40/75 °C/%RH; 7 in UDB sample showed a significantly ($p = 0.004$) lower LD content. All other samples show no significant differences to the initial samples, including the 40/75 °C/%RH; 28 samples.

CD content did not decrease significantly for 25/60 °C/%RH; 28 in brown glass and 25/60 °C/%RH; 7 in UDB, while 25/60 °C/%RH; 28 in UDB, 40/75 °C/%RH; 7 in UDB and 40/75 °C/%RH; 28 in UDB showed significantly lower CD contents.

4. Discussion

In this study, we were able to show that DPE printing in a hospital setting is feasible. Four of the five developed excipient compositions were successfully printed. The formulation P25/29-CA (plasticizer: citric acid) was not printable. Additionally, it has to be mentioned that CD did unexpectedly not tolerate the printing process, whereas the printing of LD was possible without loss.

The main goals of the study were to formulate an immediate release formulation that allows a reliable printing process within DPE. For the potential use in clinical practice, a sufficient storage stability and good hardness values to ensure personnel and therapy safety were considered crucial as well. To achieve this, different plasticizers were employed and polymer ratios were optimized.
4.1. Powder screening

Sound powder flow properties are a hallmark of high-quality pharmaceutical powders, intended to be used as an intermediate product for subsequent manufacturing processes like tableting, capsule filling and 3DP. During DPE it is crucial to ensure a consistent powder flow, since the process parameters of the melt extrusion process and the movements of the DPE printhead need to be perfectly concerted in order to guarantee an uninterrupted process.

The powder blend P25/29-M showed passable flow properties in all conducted measurements. This is to be expected regarding the sizes of API particles ($d_{50} = 51.8 \mu\text{m}$ (LD); $d_{50} = 15.3 \mu\text{m}$ (CD)) and their large quantities of 28% w/w (LD) and 7.56% w/w (CD) within the blend. On the one hand, small particles show high cohesion, which worsens the powder flow (Abdullah and Geldart, 1999). On the other hand, it is crucial to select small API particles to ensure a statistically equal distribution of the APIs in the powder blend. Additionally, it can be assumed that the small particle size and large specific surface area of the APIs promote a rapid and uniform dispersion or solution of the APIs in the polymers. Moreover, bulk density of the powder blend is low (0.46 g/mL), which is associated with high friction in the powder bed and a deterioration of the powder flow. The powder hung up during the flow time measurements in the funnel of the powder analysis device, which resembles the shape of the powder reservoir of the utilized DPE printhead. This indicated that the powder flow during the printing process would probably be insufficient as well. It was observed that the screw of the printhead created a cylindrical, core powder flow-resembling empty space between itself and the powder bed. This led to insufficient extrusion and ultimately resulted in the abortion of the printing processes. The addition of fine particulate silica as a glidant was tested. This, however, did not sufficiently enhance the powder flow. A constructed force feeder mounted onto the printhead accomplished this task (Figure 3), resulting in constant powder flow, a smooth, uninterrupted printing process and autonomous build plate adhesion of the extruded mass. Moreover, it was a key improvement in the process which ensured uniform weight (see Table 3) and content (between $100.12 \pm 1.20\%$ to $104.72 \pm 2.84\%$ for LD) of the resulting tablets.

4.2. Thermal screening

The DSC (Figure 4) and TGA (Figure 5) results suggest that no problems were to be expected with LD during the printing process, as no degradation was found up to 250 °C.

The large endothermic event observed for CD represents the release of the water of CD monohydrate. The molecular mass of anhydrous CD (226.23 g/mol) is 92.6% of the molecular weight of the monohydrate (244.24 g/mol), which corresponds well with the found reduction in mass to 92.55%. DSC confirmed the T_m . However, as CD clearly starts to decompose slightly before the T_m at about 195 °C (Figure 5), the printing temperature had to be limited in order to establish a cushion. Therefore, the aim of the printing pre-experiments was to find an excipient combination, which enables a printing temperature of at least 15 °C below the onset of the decomposition (i.e., 180 °C).

DSC measurements (Figure 6) of the polymers and mannitol confirmed literature data regarding T_g and T_m .

As expected, the glass transition of Kollidon® VA64 as well as the melting of Mannitol and Kollicoat® IR were observed in the DSC diagram of the optimized powder blend P25/29-M. The decomposition of CD was also found again, albeit at higher temperatures, whereas the release of the monohydrate is no longer visible. This was probably a result of the relatively small percentage of CD (7.56%) in the powder blend.

Lastly, the DSC diagram of the extruded filament showed some different results. There is a glass transition at about 80 °C; this reduction of Kollidon® VA64s T_g was probably a result of the added mannitol, as the addition of plasticizers is known to reduce T_g values of polymers (Honary and Orafi, 2002). Additionally, the melting peak of mannitol was not found. The plasticizer did probably not recrystallize due to the formation of a solid dispersion/solution after being melted together with the polymers. The endothermic event at the beginning of the decomposition could have been the beginning of the melting process of Kollicoat® IR, as the individual DSC of this polymer also showed a very broad melting peak, which is most probably due to the nature of polymers being blends of different chain lengths.

After dissolution, experiments showed a loss in CD. Both CD as well as the powder blend were subjected to an alternative DSC method to evaluate if the prolonged exposition to the printing temperature triggers decomposition.

DSC and TGA clearly showed that CD decomposes at distinctly lower temperatures than expected. It has to be noted that the thermogram (Figure 8) starts at about 95% mass, as the monohydrate of the CD evaporated during the initial heating phase, which is not pictured in the thermogram.

Interestingly, the isothermal DSC data of the powder blend suggests a protective effect on the CD, as no decomposition or other events were visible over the course of 30 min.

4.3. Manufacturing process and formulation screening

HPLC analysis confirmed the uniformity of the powder blend, which is crucial in order to achieve tablets of uniform content and mass.

Regarding the DPE process, three of four CQAs were achieved within the development of the formulation and manufacturing process. Consistent and reliable printability of the formulations on a glass plate, without manual aid or adhesion enhancement, was achieved through careful factorial optimization of the development process and the composition of the formulation. Moreover, the printhead was modified with the stirring device to ensure a constant material feed rate in the printhead (Figure 3). In order to be useful for compounding in a hospital pharmacy, it was seen as crucial to develop a highly automated process that requires little to no intervention from qualified personnel. This would occupy time of the qualified personnel of a hospital pharmacy. Especially printing the first layer on a glass surface without manual adhesion aid could only be achieved through careful optimization of the feed rate without over-extrusion, which would probably have resulted in bulkier tablets and weight inconsistencies. Through constant optimization of the constitution of the formulation and the shape, an immediate release profile and an outstanding hardness were achieved as well. Although extensive effort was spent on the thermal screening, only LD was able to tolerate the printing temperature, which was identified as a CPP. CD degraded partially during the printing process. Since the printing temperature was constantly monitored as a Process Analytical Technology (PAT), variations of the printing temperature were excluded for the

degradation, since the temperature of the heating element was very consistent. In consecutive experiments, filaments were extruded at lower temperatures. Unfortunately, none of the formulations offered the possibility to decrease the extrusion temperature below 150 °C, where degradation of CD was still present. Below 150 °C, the viscosity of the formulation was too high for the printer to extrude. Besides reduced CD content, an unidentified degradation product was visible during HPLC analyses. However, the dissolution data of LD shows that the process was very precise regarding the LD content of the tablets. Moreover, the immediate release profile was clearly shown. Further analysis tools such as NIR, which has just been reported as a modification for the used printer (Seoane-Viaño et al., 2023), or an in-process balance, which is now an available upgrade for the printer, could also be desirable PAT tools for further development.

Instead of using design of experiments, an iterative, factorial approach was used to develop the process, since DPE allows extremely small batches below 10 g formulation and swift changes of the process parameters through the software.

Regarding the formulation, the API amount was increased up to 35.56%, since the BCS class I APIs promote a quick dissolution of the whole formulation. Moreover, doses as high as 170/42.5 mg LD/CD require a high percentage of API to limit the size of the tablets and ensure an appreciable swallowability. Mannitol as a plasticizer has been used in the concentration of 10% for FDM printing (Windolf et al., 2021). Several different polymers were screened in advance of the study. Some of these are known to exhibit a retarding influence on the release of the API, for example, hydroxypropyl cellulose (15-35% of the tablet) [41]. Therefore, they were not viewed as suitable due to the requirement of an immediate release tablet, although some of these showed a reliable printability. Subsequently, the water-soluble polymers Kollidon® VA 64 and Kollicoat® IR were selected and used in different ratios. Kollidon® VA 64 is known as a water-soluble and brittle polymer with a low T_g (Fuenmayor et al., 2018; Shi et al., 2021; Solanki et al., 2018). Therefore, it was necessary to include a plasticizer and Kollicoat® IR as a second polymer with less brittle characteristics and a higher melt viscosity that promotes adhesion on the built plate during extrusion (Kolter et al., 2012). Its acceptable water solubility is an important aspect for the formulation's immediate release characteristic. Moreover, Kollicoat® IR's flexible character improved the hardness characteristics of the tablet and reduces their friability. Only a combination of both polymers led to the fulfillment of all these characteristics.

During this study, the ratios of the polymers were optimized to achieve reliable printability through an ideal melt viscosity, a quick disintegration and sufficient tablet hardness. The polymer ratio P25/29-M proved to provide a quick tablet disintegration as well as the most reliable printing process. P25/29-M was preferred to P25/29-CSM, since the latter did not show a faster disintegration, while the included Compressol® SM (co-processed Sorbitol and Mannitol) might increase the formulations vulnerability towards humidity since sorbitol is more hygroscopic than mannitol (Chen et al., 2020; Rice et al., 2020). P25/29-M was therefore selected exclusively for further development and optimization of the different shapes. P25/29-CA could not be extruded, since the sample's viscosity was too high for the screw to extrude the formulation. The plasticizing effect of citric acid has been demonstrated for hot melt extrusion, although higher concentrations than 10% were found to show a greater effect (Schilling et al., 2010).

Over the course of disintegration experiments, the tablets formed a sphere-like shape. This prolonged the disintegration time, as a sphere combines maximal volume with minimal surface. Consequently, the Donut shape was introduced. The hole in the middle of the tablet increases the SA/V ratio and prevents the mechanistic formation of a sphere. Finally, the Oblongs were printed and showed the most noticeable results in disintegration experiments. Resulting from their reduced infill, they offer the highest specific surface of all tablets.

4.4. Hardness

The DPE printing process, the selected tablet excipients and their employed quantities differ vastly from conventionally manufactured compacted tablets. Conventional tablets are compacted out of powder or granules with high compaction force, which creates solid bonds between the powder particles where brittle fragmentation, plastic and elastic deformation play a role (Humbert Droz et al., 1983; Nordström et al., 2012; York, 1992). DPE printed tablets gain their hardness through solidification of the melt-extruded mass without compaction. Overall, the tablets show very appealing hardness values. Especially the addition of the more flexible polymer Kollicoat® IR and the plasticizer mannitol should be responsible for the increase in hardness as well as the reduction of the formulation's brittleness, which leads to

decreased friability (Gong and Sun, 2015). Decreased friability is especially important for a tablet that was developed to be used in a hospital setting, since the personnel is exposed to the tablet through manual handling without primary packaging during manufacturing, packaging and administration to the patient. To account for a worst-case scenario, only the small Donuts and the corresponding large shape were evaluated in friability testing, since the small Donuts showed the lowest crushing strengths.

As expected, the Cylinders show the highest resistance to crushing values. The Donuts and Oblongs show lower hardness values than the Cylinders, which are nonetheless very satisfying. Since both forms lack some stability because of empty space within the shape through the hole or reduced infill, they brake at lower forces. The friability results of the Donuts were very convincing and considered sufficient. In conclusion, the other formulations were not tested.

4.5. Disintegration

Due to its considerably lower time and material consumption than dissolution experiments, disintegration testing was used as a surrogate method for quickly screening all printable formulations for their potential to produce immediate release tablets (Fu et al., 2020; Nickerson et al., 2018), which was identified as a CQA.

The formulations mainly consist of water-soluble polymers and, as a result of the manufacturing process, most likely exhibit a minimal porosity of the individual extrudate strands. Therefore, no disintegration typical for compacted tablets was expected but more of an erosion process of the slightly swelling surface, comparable to lozenges. This expectation was met and led to the introduction of the disintegration rate, which enables a better comparison of the different formulations while additionally being a rough guide for their dissolution time.

Most of the tablets stuck to the respective discs, due to swelling of the surface. This reduced the surface area that is in contact with the disintegration medium and thereby most likely decelerated the process. Additionally, the discs have holes and the tablets did not adhere uniformly, which resulted in differing influences on the singular tablets and thereby increased the standard deviations of the respective mean disintegration times. The large Oblongs were the only tablets that did not stick to the discs, which means that the disintegration tests of these were influenced to a lesser degree. Disintegration testing was solely considered a screening method, so disintegration times were considered promising. The Ph. Eur. (Chapter 5.17.1) mentions the release of at least 80% of the API in 45 min or less as a general acceptance criterion for immediate release tablets (EDQM, 2021). Considering the mean disintegration times (< 54 min), even if potentially negatively influenced, it seems likely that every screened formulation could yield an immediate release tablet.

The interchange of the plasticizer mannitol to Compressol® SM did not exhibit an influence on the disintegration rate. Therefore, P25/29-M was considered the most auspicious powder blend, as it exhibited the best printability and every formulation showed promising disintegration times.

Hence, P25/29-M was selected as the powder blend, which would be used to examine the influence of the tablet shape. As expected, the Donut resulted in an accelerated disintegration, which became especially obvious for the large tablets, as the disintegration rate was significantly higher than that of the large Cylinders of every other powder blend. When the Oblongs were examined, the acceleration was even more distinct. The large Oblongs disintegrated significantly faster than the small tablets of every other formulation, which is equally shown in their significantly higher disintegration rate.

These results show the immense influence that is exerted by the different tablet shapes. However, this had to be expected, as the Donuts and Oblongs have a higher SA/V ratio than the Cylinders. Ultimately, this strengthens the position of 3DP in tablet manufacturing, as the oblong shape with a reduced infill cannot be produced by classical tableting via compaction.

4.6. Dissolution & Content analysis

Dissolution data shows that it is possible to manufacture immediate release tablets with DPE. Four of the six investigated formulations released more than 85% of the LD in less than 15 min. This is particularly appealing, because a BCS-based biowaiver approach defines these values as a threshold at which an f2 comparison is unnecessary to demonstrate similarity between two products (ICH, 2020). Still,

although the dissolution was considerably slower, the other two formulations are to be considered immediate release formulations, as they released more than 80% of the LD in less than 45 min (EDQM, 2021) (see section 4.5.). With an f_2 -value of 55.30 between the large Donuts and Cylinders, these formulations can be considered similar regarding the release of LD.

Unfortunately, the printing process seemed to trigger the decomposition of CD, as only about 60-70% were recovered from the completely dissolved tablets, although LD was recovered completely. Therefore, it was found necessary to further evaluate the thermal stability of CD (Section 4.2.). Nonetheless, the dissolution behavior of the remaining CD seemed to be comparable to that of LD, which had to be expected as both substances are BCS class I drugs.

Ultimately, it was expected that the different shapes exhibit a considerable influence on the dissolution behavior, due to their different SA/V ratio and disintegration results and that the influence would be more apparent with larger tablets. These expectations were thoroughly confirmed, as the time needed to release 80% of the LD from the large Oblongs was about a quarter of the time needed for the large Cylinders.

After identifying the decomposition of CD, it was found necessary to investigate if the alternative DOPA decarboxylase inhibitor BZ tolerates the printing process. The extrusion experiments with BZ showed that it seems to be even more thermolabile than CD. More than 70% of the substance was lost during extrusion, compared to 30-40% of the CD that was lost at much higher extrusion temperatures. Therefore, BZ was not viewed as an alternative and no further experiments were conducted.

4.7. Stability analysis

The stability test gathered valuable data regarding the formulation's vulnerability towards increased humidity and temperature.

LD content of 40/75; 7 in UDB decreased significantly. This was most likely caused by a slightly lower weight of the three samples (average weight 207.7 mg) compared to the other samples (average weight 216.9 mg). Moreover, the 40/75; 28 in UDB showed no significantly lower content, despite having been exposed to the most stressful conditions for the longest time. This leads to the conclusion that LD should tolerate both conditions and packagings for at least 28 days. This is completely sufficient for the intended clinical supply with CLMM, where tablets would be printed daily according to the patient's needs.

CD showed moderate stability if packed in brown glass and in the mildest storage condition 25/60; 7 in UDB. In 25/60; 28 in UDB and in both accelerated condition samples, meaningful amounts of Carbidopa degraded during the study. It has been shown that carbidopa is vulnerable to degradation processes such as oxidation and hydrolysis (Choudhary, 2018; Subramanian et al., 2020). The manufacturer of the UDBs investigated their moisture permeability thoroughly (Akasaki, 2016). According to these investigations, 3-15 g/m³ permeates the UDBs at 20 °C / 60% RH and 30 °C / 90% RH in 24 h, respectively. This exposure, which should be lower or absent in the brown glass packaging, led to a significant decrease of CD content. However, the 25/60; 7 in UDB indicates that CD is stable enough for the intended use in CLMM, since the tablets are prepared daily and storage is very short for personalized tablets. Moreover, the pharmacy's environment must be monitored and kept under 25 °C.

5. Conclusions

It was possible to develop an excipient composition that enables reliable DPE printing without baseplate modifications or baseplate heating. The printed tablets are characterized by an immediate release and outstanding hardness values; the latter make them particularly suitable for inpatient care of a hospital with CLMM, which is exemplified by a sufficient storage stability.

Thus, the implementation of DPE into the CLMM is feasible. However, the model APIs showed that not every substance is suited for the DPE technique, as, in contrast to LD, CD did not tolerate the manufacturing process. This was unexpected, as careful thermal screening was carried out prior to formulation experiments. This highlights the importance of CPPs and CMAs during the early development stages and the risk assessment. Finally, other BCS class I APIs with sufficient thermal stability should be printable with the optimized formulation.

Patents

As a result of this project, the patent application EP23156479.0 was filed on February 14th, 2023.

Supplementary Materials

All data is presented within this manuscript.

CRedit authorship contribution statement

Moritz Rosch: Conceptualization, Data curation, Formal analysis, Funding acquisition, Investigation, Methodology, Project administration, Resources, Software, Supervision, Validation Visualization, Writing - original draft, Writing - review & editing. **Tobias Gutowski:** Conceptualization, Data curation, Formal analysis, Funding acquisition, Investigation, Methodology, Project administration, Resources, Software, Supervision, Validation Visualization, Writing - original draft, Writing - review & editing. **Michael Baehr:** Conceptualization, Funding acquisition, Project administration, Resources, Supervision, Writing - review & editing. **Jan Eggert:** Conceptualization, Funding acquisition, Project administration, Resources, Writing - review & editing. **Karl Gottfried:** Conceptualization, Methodology, Writing - review & editing. **Christopher Gundler:** Conceptualization, Funding acquisition, Writing - review & editing. **Sylvia Nürnberg:** Conceptualization, Supervision, Writing - review & editing. **Claudia Langebrake:** Conceptualization, Funding acquisition, Supervision, Writing - review & editing. **Adrin Dadkhah:** Conceptualization, Data curation, Formal analysis, Funding acquisition, Investigation, Methodology, Project administration, Resources, Software, Visualization, Writing - original draft, Writing - review & editing.

Funding

The study is part of a project that was funded by the European Regional Development Fund (ERDF) of the European Union. It presents a proof of concept for the implementation of pharmaceutical 3DP in the already existing CLMM of a hospital pharmacy.

Informed Consent Statement

Not applicable.

Data Availability Statement

All data is contained in the article.

Acknowledgments

The authors would like to thank their colleagues of the hospital pharmacy for their constant support during the project. Special thanks go to Thomas Schoch, who supported the authors with the technical modifications of the 3D printer. Moreover, the authors thank Alvaro Goyanes and the team of FabRx Ltd. for productive conversations and their technical support. We thank AK Langguth of Johannes Gutenberg University Mainz as well as AG Leopold and AG Luinstra of Universität Hamburg for support with devices and experiments. Especially Sophie Luise Meiser, Valentin Stahl, Cristian Kulcitki and Stefan Bleck have to be mentioned. Additionally, Erik Wollmer for his input on HPLC methods. Lastly, the authors thank the companies, which are mentioned in the materials section, for their donated samples throughout this project.

Declaration of Competing Interest

The authors declare that they have no known competing financial interests or personal relationships that could have appeared to influence the work reported in this paper.

References Carbidopa.

- Abdullah, E.C., Geldart, D., 1999. The use of bulk density measurements as flowability indicators. *Powder Technology* 102, 151-165.
- Ajit, V.K., Arun, G.K., Piush, K., Rakesh, P., 2018. Formulation and Development of Floating Microspheres containing Levodopa and Carbidopa. *Asian Journal of Pharmacy and Technology* 8, 200-202.
- Akasaki, N., 2016. Spec P160_P2010 Ref. No. YFPF20160616. Yuyama Co, Ltd., p. 2.
- Baehr, M., Melzer, S., 2018. Closed Loop Medication Management: Arzneimitteltherapiesicherheit im Krankenhaus, 1. Edition ed. MWV Medizinisch Wissenschaftliche Verlagsgesellschaft, Berlin, Germany.
- Bayoumy, K., Gaber, M., Elshafeey, A., Mhaimed, O., Dineen, E.H., Marvel, F.A., Martin, S.S., Muse, E.D., Turakhia, M.P., Tarakji, K.G., Elshazly, M.B., 2021. Smart wearable devices in cardiovascular care: where we are and how to move forward. *Nat Rev Cardiol* 18, 581-599.
- Berger, V., Sommer, C., Boje, P., Hollmann, J., Hummelt, J., König, C., Lezius, S., van der Linde, A., Marhenke, C., Melzer, S., Michalowski, N., Baehr, M., Langebrake, C., 2022. The impact of pharmacists' interventions within the Closed Loop Medication Management process on medication safety: An analysis in a German university hospital. *Front Pharmacol* 13, 1030406.
- Boniatti, J., Januskaite, P., Fonseca, L.B.d., Viçosa, A.L., Amendoeira, F.C., Tuleu, C., Basit, A.W., Goyanes, A., Ré, M.-I., 2021. Direct Powder Extrusion 3D Printing of Praziquantel to Overcome Neglected Disease Formulation Challenges in Paediatric Populations. *Pharmaceutics* 13.
- Bruno, E., Viana, P.F., Sperling, M.R., Richardson, M.P., 2020. Seizure detection at home: Do devices on the market match the needs of people living with epilepsy and their caregivers? *Epilepsia* 61.
- Buhmann, C., Bihler, M., Emich, K., Hidding, U., Pötter-Nerger, M., Gerloff, C., Niessen, A., Flügel, T., Koseki, J.-C., Nienstedt, J.C., Pflug, C., 2019. Pill swallowing in Parkinson's disease: A prospective study based on flexible endoscopic evaluation of swallowing. *Parkinsonism & Related Disorders* 62, 51-56.
- Carr, R.L., 1965. Evaluating flow properties of solids. *Chemical Engineering* 72, 163-168.
- Chamberlain, R., Windolf, H., Geissler, S., Quodbach, J., Breitreutz, J., 2022. Precise Dosing of Pramipexole for Low-Dosed Filament Production by Hot Melt Extrusion Applying Various Feeding Methods. *Pharmaceutics* 14, 216.
- Chen, M., Zhang, W., Wu, H., Guang, C., Mu, W., 2020. Mannitol: physiological functionalities, determination methods, biotechnological production, and applications. *Applied Microbiology and Biotechnology* 104, 6941-6951.
- Choudhary, A.N.C., Ajay, Dutta, Kamlesh K, 2018. Forced degradation study and validation of a RP-HPLC method for simultaneous estimation for drug content and release of Levodopa, Carbidopa and Entacapone in combined dosage form. *The Pharma Innovation Journal* 7, 14.
- Díaz-Torres, E., Suárez-González, J., Monzón-Rodríguez, C.N., Santoveña-Estévez, A., Fariña, J.B., 2023. Characterization and Validation of a New 3D Printing Ink for Reducing Therapeutic Gap in Pediatrics through Individualized Medicines. *Pharmaceutics* 15, 1642.
- EDQM, 2021. European Pharmacopoeia, 10 ed. Deutscher Apotheker Verlag, Stuttgart, Germany.
- Fell, J.T., Newton, J.M., 1968. The tensile strength of lactose tablets. *Journal of Pharmacy and Pharmacology* 20, 657-659.
- Forough, A.S., Wong, S.Y.M., Lau, E.T.L., Santos, J.M.S., Kyle, G.J., Steadman, K.J., Cichero, J.A.Y., Nissen, L.M., 2018. Nurse experiences of medication administration to people with swallowing difficulties living in aged care facilities: a systematic review of qualitative evidence. *JB Database System Rev Implement Rep* 16, 71-86.
- Fox, S.H., Katzenschlager, R., Lim, S.Y., Barton, B., de Bie, R.M.A., Seppi, K., Coelho, M., Sampaio, C., Committee, M.D.S.E.-B.M., 2018. International Parkinson and movement disorder society evidence-based medicine review: Update on treatments for the motor symptoms of Parkinson's disease. *Mov Disord* 33, 1248-1266.
- Fu, M., Al-Gousous, J., Blechar, J.A., Langguth, P., 2020. Enteric Hard Capsules for Targeting the Small Intestine: Positive Correlation between In Vitro Disintegration and Dissolution Times. *Pharmaceutics* 12, 123-123.
- Fuenmayor, E., Forde, M., Healy, A.V., Devine, D.M., Lyons, J.G., McConville, C., Major, I., 2018. Material considerations for fused-filament fabrication of solid dosage forms. *Pharmaceutics* 10, 44.
- Gong, X., Sun, C.C., 2015. A new tablet brittleness index. *European Journal of Pharmaceutics and Biopharmaceutics* 93, 260-266.
- Goyanes, A., Allahham, N., Trenfield, S.J., Stoyanov, E., Gaisford, S., Basit, A.W., 2019. Direct powder extrusion 3D printing: Fabrication of drug products using a novel single-step process. *International Journal of Pharmaceutics* 567, 118471.
- Goyanes, A., Buanz, A.B.M., Hatton, G.B., Gaisford, S., Basit, A.W., 2015a. 3D printing of modified-release aminosalicylate (4-ASA and 5-ASA) tablets. *European Journal of Pharmaceutics and Biopharmaceutics* 89, 157-162.
- Goyanes, A., Robles Martinez, P., Buanz, A., Basit, A.W., Gaisford, S., 2015b. Effect of geometry on drug release from 3D printed tablets. *International Journal of Pharmaceutics* 494, 657-663.

- Hoffmann, L., Breikreutz, J., Quodbach, J., 2022. Fused Deposition Modeling (FDM) 3D Printing of the Thermo-Sensitive Peptidomimetic Drug Enalapril Maleate. *Pharmaceutics* 14, 2411.
- Honary, S., Orafi, H., 2002. The Effect of Different Plasticizer Molecular Weights and Concentrations on Mechanical and Thermomechanical Properties of Free Films. *Drug Development and Industrial Pharmacy* 28, 711-715.
- Humbert Droz, P., Gurny, R., Mordier, D., Doelker, E., 1983. Densification behaviour of drugs presenting availability problems. *International Journal of Pharmaceutical Technology and Product Manufacture* 4, 29-35.
- ICH, 2003. ICH Topic Q 1 A (R2) Stability Testing of new Drug Substances and Products. European Medicines Agency.
- ICH, 2009. ICH Q8 (R2) Pharmaceutical development - Scientific guideline. European Medicines Agency.
- ICH, 2020. ICH M9 guideline on biopharmaceutics classification system-based biowaivers. European Medicines Agency.
- ICH, 2022. ICH guideline Q2(R2) on validation of analytical procedures. European Medicines Agency.
- Jüptner, A.C., 2022. title. Monograph, Kiel University.
- Kim, D.W., Zavala, E., Kim, J.K., 2020. Wearable technology and systems modeling for personalized chronotherapy. *Current Opinion in Systems Biology* 21, 9-15.
- Kissi, E.O., Nilsson, R., Nogueira, L.P., Larsson, A., Tho, I., 2021. Influence of Drug Load on the Printability and Solid-State Properties of 3D-Printed Naproxen-Based Amorphous Solid Dispersion. *Molecules* 26.
- Kolter, K., Karl, M., Gryczke, A., 2012. Hot-Melt Extrusion with BASF Pharma Polymers, 2nd Revised and Enlarged Edition ed. BASF SE.
- Krueger, L., Cao, Y., Zheng, Z., Ward, J., Miles, J.A., Papat, A., 2023. 3D printing tablets for high-precision dose titration of caffeine. *International Journal of Pharmaceutics* 642, 123132.
- Langebrake, C., Gottfried, K., Dadkhah, A., Eggert, J., Gutowski, T., Rosch, M., Schönbeck, N., Gundler, C., Nürnberg, S., Ückert, F., Baehr, M., 2023. Patient-individual 3D-printing of drugs within a machine-learning-assisted closed-loop medication management – Design and first results of a feasibility study. *Clinical eHealth* 6, 3-9.
- Ledeti, A., Olariu, T., Caunii, A., Vlase, G., Circioban, D., Baul, B., Ledeti, I., Vlase, T., Murariu, M., 2018. Evaluation of thermal stability and kinetic of degradation for levodopa in non-isothermal conditions. *Journal of Thermal Analysis and Calorimetry* 131, 1881-1888.
- Liang, E., Wang, Z., Li, X., Wang, S., Han, X., Chen, D., Zheng, A., 2023. 3D Printing Technology Based on Versatile Gelatin-Carrageenan Gel System for Drug Formulations. *Pharmaceutics* 15.
- Madathilethu, J., Roberts, M., Peak, M., Blair, J., Prescott, R., Ford, J.L., 2018. Content uniformity of quartered hydrocortisone tablets in comparison with mini-tablets for paediatric dosing. *BMJ Paediatrics Open* 2, e000198.
- Moore, J.W., Flanner, H.H., 1996. Mathematical comparison of dissolution profiles. *Pharmaceutical technology* 20, 64-74.
- Nickerson, B., Kong, A., Gerst, P., Kao, S., 2018. Correlation of dissolution and disintegration results for an immediate-release tablet. *Journal of Pharmaceutical and Biomedical Analysis* 150, 333-340.
- Nordström, J., Klevan, I., Alderborn, G., 2012. A protocol for the classification of powder compression characteristics. *European Journal of Pharmaceutics and Biopharmaceutics* 80, 209-216.
- Ong, J.J., Awad, A., Martorana, A., Gaisford, S., Stoyanov, E., Basit, A.W., Goyanes, A., 2020. 3D printed opioid medicines with alcohol-resistant and abuse-deterrent properties. *International Journal of Pharmaceutics* 579, 119169.
- Pahwa, R., Bergquist, F., Horne, M., Minshall, M.E., 2020. Objective measurement in Parkinson's disease: a descriptive analysis of Parkinson's symptom scores from a large population of patients across the world using the Personal KinetiGraph®. *Journal of Clinical Movement Disorders* 7.
- Pflieger, T., Venkatesh, R., Dachtler, M., Eggenreich, K., Laufer, S., Lunter, D., 2022. Novel Approach to Pharmaceutical 3D-Printing Omitting the Need for Filament—Investigation of Materials, Process, and Product Characteristics. *Pharmaceutics* 14.
- Powers, R., Etezadi-Amoli, M., Arnold, E.M., Kianian, S., Mance, I., Gibiansky, M., Trietsch, D., Alvarado, A.S., Kretlow, J.D., Herrington, T.M., Brillman, S., Huang, N., Lin, P.T., Pham, H.A., Ullal, A.V., 2021. Smartwatch inertial sensors continuously monitor real-world motor fluctuations in Parkinson's disease. *Sci Transl Med* 13.
- Raut, P.P., Charde, S.Y., 2014. Simultaneous estimation of levodopa and carbidopa by RP-HPLC using a fluorescence detector: its application to a pharmaceutical dosage form. *Luminescence* 29, 762-771.
- Rice, T., Zannini, E., K. Arendt, E., Coffey, A., 2020. A review of polyols – biotechnological production, food applications, regulation, labeling and health effects. *Critical Reviews in Food Science and Nutrition* 60, 2034-2051.
- Rodríguez-Pombo, L., Awad, A., Basit, A.W., Alvarez-Lorenzo, C., Goyanes, A., 2022. Innovations in Chewable Formulations: The Novelty and Applications of 3D Printing in Drug Product Design. *Pharmaceutics* 14, 1732.

- Schilling, S.U., Shah, N.H., Malick, A.W., Infeld, M.H., McGinity, J.W., 2010. Citric acid as a solid-state plasticizer for Eudragit RS PO. *Journal of Pharmacy and Pharmacology* 59, 1493-1500.
- Seoane-Viaño, I., Januskaite, P., Alvarez-Lorenzo, C., Basit, A.W., Goyanes, A., 2021a. Semi-solid extrusion 3D printing in drug delivery and biomedicine: Personalised solutions for healthcare challenges. *Journal of Controlled Release* 332, 367-389.
- Seoane-Viaño, I., Trenfield, S.J., Basit, A.W., Goyanes, A., 2021b. Translating 3D printed pharmaceuticals: From hype to real-world clinical applications. *Advanced Drug Delivery Reviews* 174, 553-575.
- Seoane-Viaño, I., Xu, X., Ong, J.J., Teyeb, A., Gaisford, S., Campos-Álvarez, A., Stulz, A., Marcuta, C., Kraschew, L., Mohr, W., Basit, A.W., Goyanes, A., 2023. A case study on decentralized manufacturing of 3D printed medicines. *International Journal of Pharmaceutics*: X 5, 100184.
- Shi, K., Slavage, J.P., Maniruzzaman, M., Nokhodchi, A., 2021. Role of release modifiers to modulate drug release from fused deposition modelling (FDM) 3D printed tablets. *International Journal of Pharmaceutics* 597, 120315-120315.
- Solanki, N.G., Tahsin, M., Shah, A.V., Serajuddin, A.T.M., 2018. Formulation of 3D Printed Tablet for Rapid Drug Release by Fused Deposition Modeling: Screening Polymers for Drug Release, Drug-Polymer Miscibility and Printability. *Journal of Pharmaceutical Sciences* 107, 390-401.
- Subramanian, V.B., Konduru, N., Katari, N.K., Dongala, T., Gundla, R., 2020. A simple high-performance liquid chromatography method development for Carbidopa and Levodopa impurities: Evaluation of risk assessment before method validation by Quality by Design approach. *Sep Sci Plus* 3, 530-539.
- Tagami, T., Ito, E., Kida, R., Hirose, K., Noda, T., Ozeki, T., 2021. 3D printing of gummy drug formulations composed of gelatin and an HPMC-based hydrogel for pediatric use. *International Journal of Pharmaceutics* 594, 120118.
- Vaz, V.M., Kumar, L., 2021. 3D Printing as a Promising Tool in Personalized Medicine. *AAPS PharmSciTech* 22, 49.
- Vinks, A.A., Peck, R.W., Neely, M., Mould, D.R., 2019. Development and Implementation of Electronic Health Record-Integrated Model-Informed Clinical Decision Support Tools for the Precision Dosing of Drugs. *Clinical Pharmacology & Therapeutics* 107, 129-135.
- Windolf, H., Chamberlain, R., Quodbach, J., 2021. Predicting Drug Release from 3D Printed Oral Medicines Based on the Surface Area to Volume Ratio of Tablet Geometry. *Pharmaceutics* 13.
- Yan, T.T., Lv, Z.F., Tian, P., Lin, M.M., Lin, W., Huang, S.Y., Chen, Y.Z., 2020. Semi-solid extrusion 3D printing ODFs: an individual drug delivery system for small scale pharmacy. *Drug Dev Ind Pharm* 46, 531-538.
- York, P., 1992. Crystal engineering and particle design for the powder compaction process. *Drug Development and Industrial Pharmacy* 18, 677-721.
- Yu, I., Chen, R.K., 2020. A Feasibility Study of an Extrusion-Based Fabrication Process for Personalized Drugs. *J Pers Med* 10.
- Yu, L.X., Amidon, G., Khan, M.A., Hoag, S.W., Polli, J., Raju, G.K., Woodcock, J., 2014. Understanding pharmaceutical quality by design. *AAPS Journal* 16, 771-783.
- Zhu, C., Tian, Y., Zhang, E., Gao, X., Zhang, H., Liu, N., Han, X., Sun, Y., Wang, Z., Zheng, A., 2022. Semisolid Extrusion 3D Printing of Propranolol Hydrochloride Gummy Chewable Tablets: an Innovative Approach to Prepare Personalized Medicine for Pediatrics. *AAPS PharmSciTech* 23, 166.

Figure Captions

Figure 1: 3D printed PLA sinker, scale in cm

Figure 2: Pictures of DPE printed tablets, scale in cm; a): small and large cylinder of P20/34-M, P25/29-M, P30/24-M and P25/29-CSM. b): Donuts and Oblongs of P25/29-M

Figure 3: DPE printhead, modified with force feeder

Figure 4: DSC diagrams of the APIs (only first heating cycle); top - LD, bottom – CD

Figure 5: TGA thermogram of the APIs

Figure 6: DSC Diagrams of the excipients (only first heating cycle), powder blend and filament; top to bottom: Kollicoat[®] IR, Kollidon[®] VA64, Mannitol, powder blend, filament

Figure 7: Isothermal (182 °C) section of DSC runs (exotherm up); top - CD, bottom - powder blend

Figure 8: Isothermal (180 °C) TGA thermogram of CD

Figure 9: Dissolution diagram (LD) of the six different tablets of formulation P25/29-M (n = 6)

Figure 10: Dissolution diagram (CD) of the six different tablet of formulation P25/29-M (n = 6)

Tables

Table 1: Formulations evaluated during the study

Formulation	Levodopa [%]	Carbidopa [%]	Kollidon® VA64 [%]	Kollicoat® IR [%]	Plasticizer [%]
P20/34-M	28	7.56	20	34.44	10 (Mannitol)
P25/29-M	28	7.56	25	29.44	10 (Mannitol)
P30/24-M	28	7.56	30	24.44	10 (Mannitol)
P25/29-CSM	28	7.56	25	29.44	10 (Compressol® SM)
P25/29-CA	28	7.56	25	29.44	10 (Citric acid)

Table 2: Crushing strengths of all tablet shapes of Formulation P25/29-M in descending order

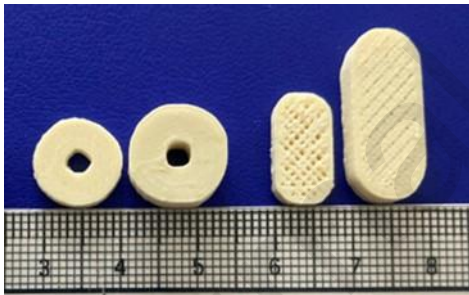
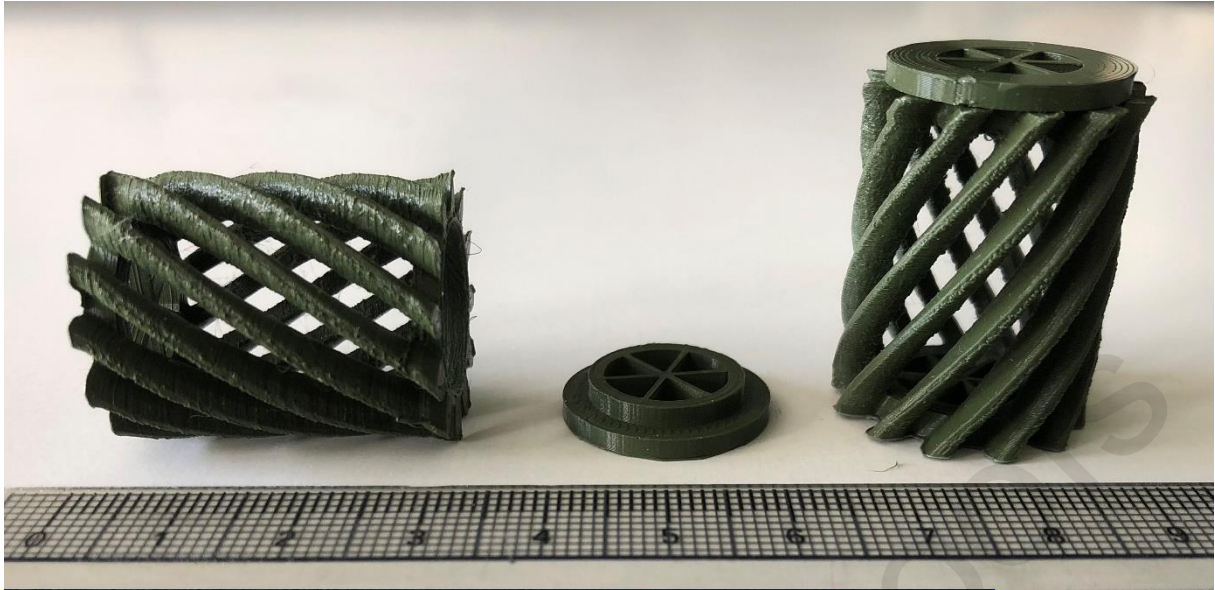
Shape – Size	Crushing strength ± SD [N]
Cylinder – large	465.5 ± 58.3
Cylinder – small	236.5 ± 70.5
Donut – large	172.9 ± 21.7
Oblong – large	131.7 ± 30.8
Oblong – small	107.0 ± 10.7
Donut – small	62.0 ± 18.3

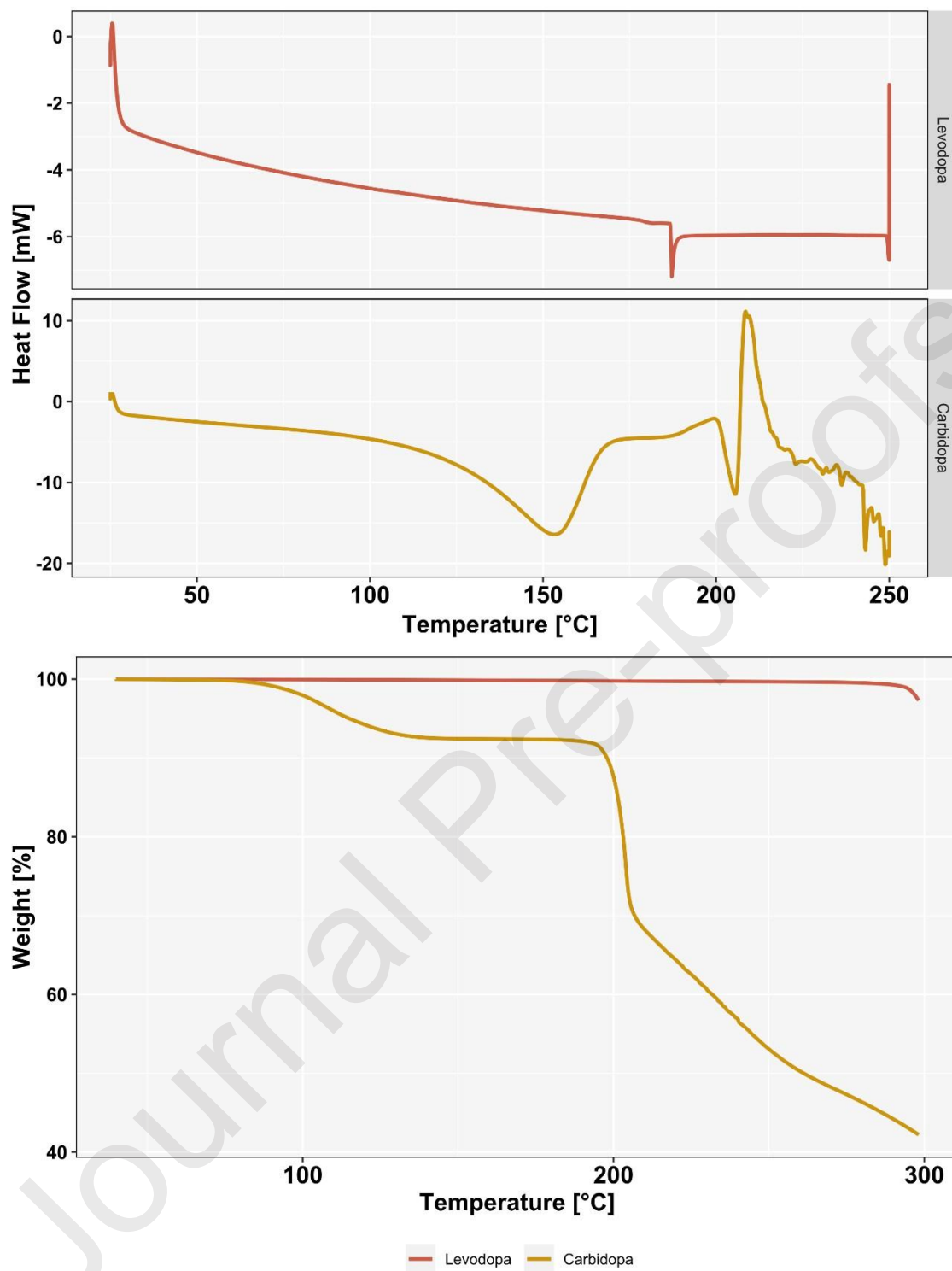
Table 3: Disintegration data of the different constitutions and shapes (n = 6)

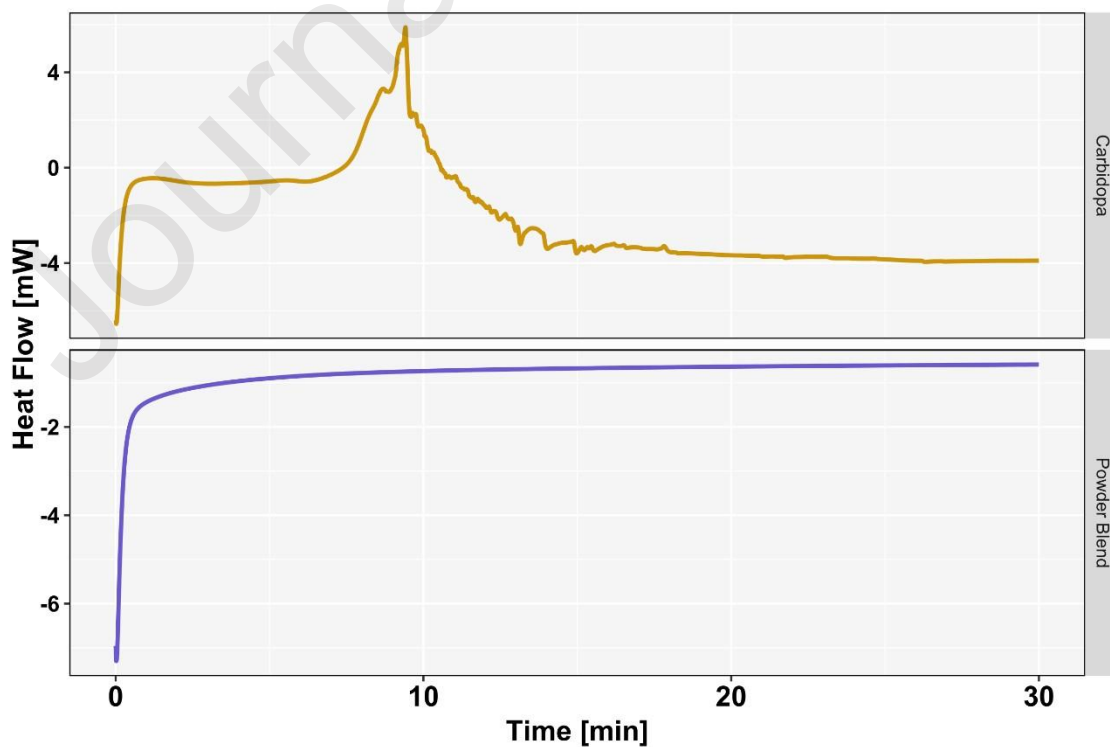
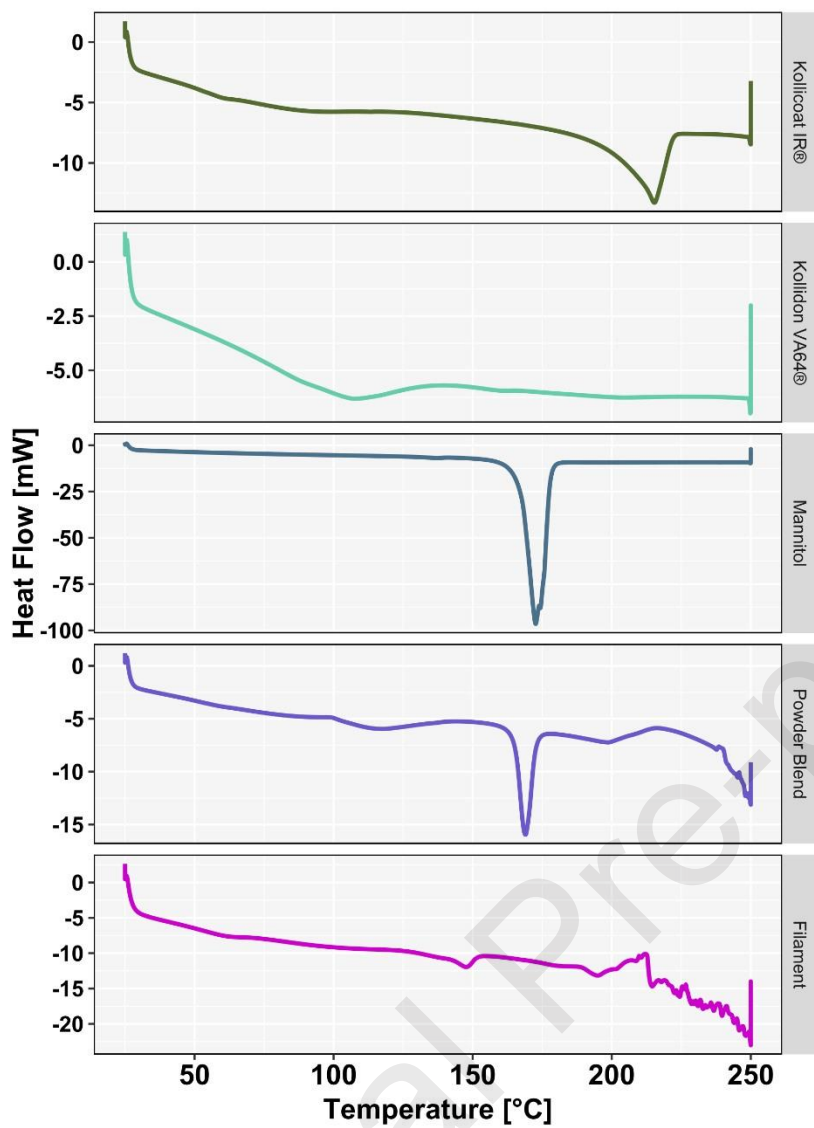
Formulation	Shape	Tablet weight \pm SD [mg]	Disintegration time \pm SD [mm:ss]	Disintegration rate \pm SD [mg/s]
P20/34-M	Cylinder	216.62 \pm 6.81	1363 \pm 195	0.16 \pm 0.02
		610.07 \pm 9.21	2562 \pm 546	0.25 \pm 0.05
P25/29-M	Cylinder	216.78 \pm 4.90	1285 \pm 214	0.17 \pm 0.04
		603.50 \pm 7.44	3189 \pm 274	0.19 \pm 0.02
	Donut	209.93 \pm 3.75	1362 \pm 78	0.15 \pm 0.01
		616.95 \pm 16.69	1756 \pm 384	0.36 \pm 0.07
	Oblong	227.08 \pm 2.30	762 \pm 107	0.30 \pm 0.05
		598.57 \pm 6.85	689 \pm 104	0.89 \pm 0.15
P30/24-M	Cylinder	216.08 \pm 4.96	1678 \pm 154	0.13 \pm 0.01
		588.67 \pm 4.44	3223 \pm 395	0.19 \pm 0.02
P25/29-CSM	Cylinder	225.78 \pm 7.99	1324 \pm 145	0.17 \pm 0.02
		620.58 \pm 6.88	3226 \pm 103	0.19 \pm 0.01

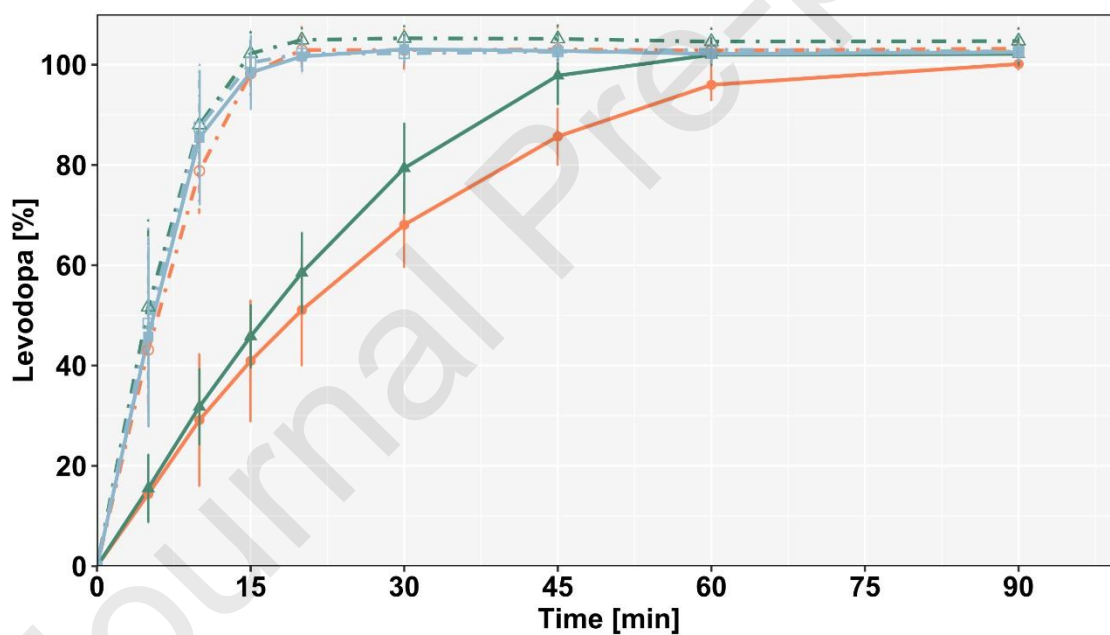
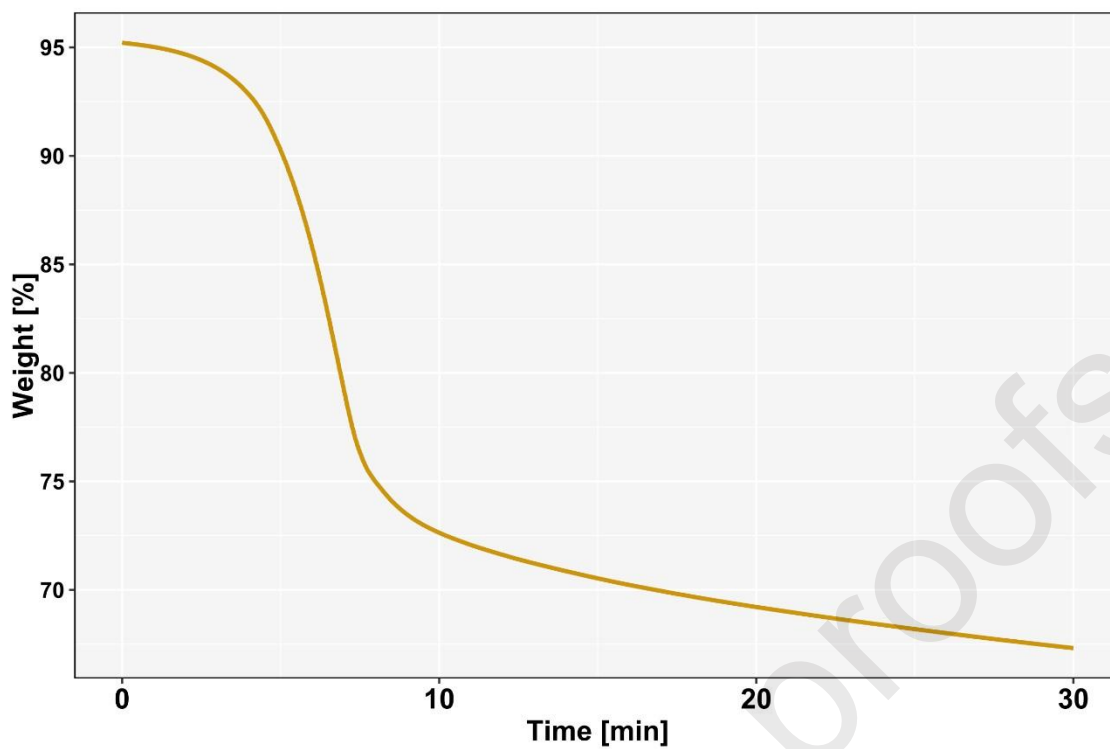
Table 4: LD and CD contents (mean \pm SD) of small Donuts of P25/29-M, measured after storage in different conditions in different packaging (UDB = Unit Dose Bag).

Storage condition and packaging [°C/%RH; days]	Levodopa content [%]	Carbidopa content [%]
Post-production values	104.72 \pm 2.84	64.91 \pm 1.54
25/60; 7 in UDB	101.48 \pm 1.23	61.31 \pm 1.40
25/60; 28 in UDB	103.26 \pm 2.08	57.00 \pm 5.12
25/60; 28 in brown glass	103.65 \pm 2.10	62.33 \pm 1.82
40/75; 7 in UDB	97.84 \pm 0.39	52.87 \pm 0.58
40/75; 28 in UDB	101.95 \pm 1.83	46.97 \pm 2.02



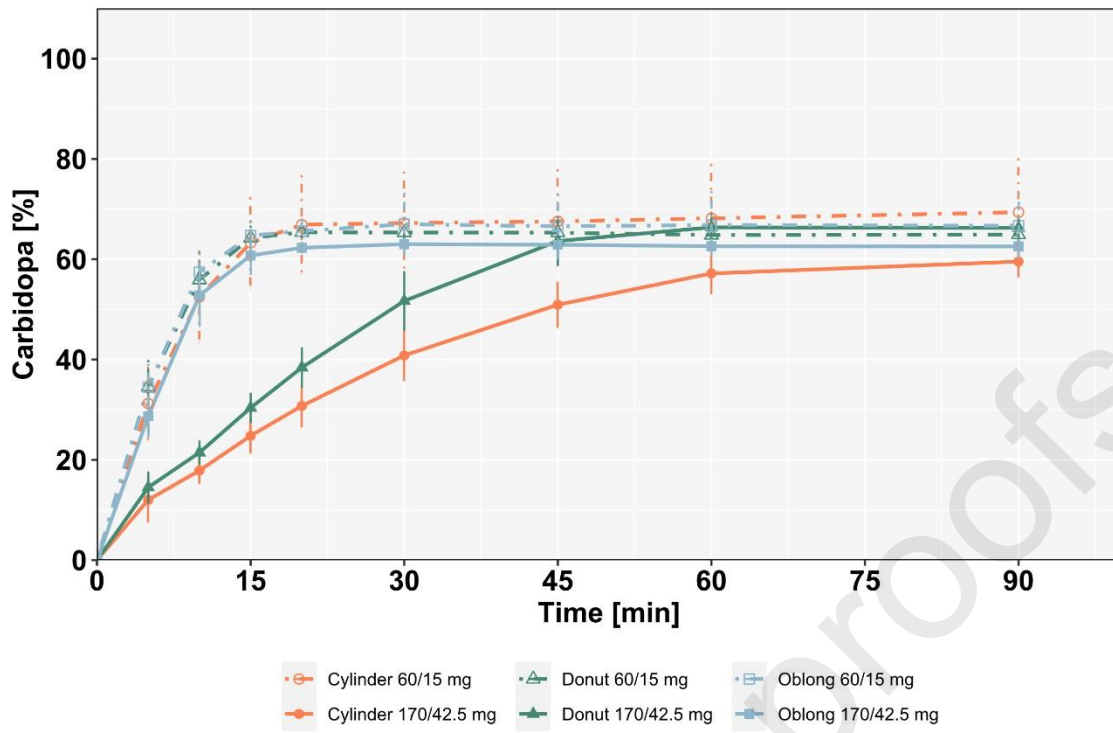






Legend for Levodopa [%] vs Time [min]:

- Cylinder 60/15 mg (Red circle)
- Donut 60/15 mg (Green triangle)
- Oblong 60/15 mg (Blue square)
- Cylinder 170/42.5 mg (Orange circle)
- Donut 170/42.5 mg (Dark green triangle)
- Oblong 170/42.5 mg (Dark blue square)



CRedit authorship contribution statement

Moritz Rosch: Conceptualization, Data curation, Formal analysis, Funding acquisition, Investigation, Methodology, Project administration, Resources, Software, Supervision, Validation Visualization, Writing - original draft, Writing - review & editing. **Tobias Gutowski:** Conceptualization, Data curation, Formal analysis, Funding acquisition, Investigation, Methodology, Project administration, Resources, Software, Supervision, Validation Visualization, Writing - original draft, Writing - review & editing. **Michael Baehr:** Conceptualization, Funding acquisition, Project administration, Resources, Supervision, Writing - review & editing. **Jan Eggert:** Conceptualization, Funding acquisition, Project administration, Resources, Writing - review & editing. **Karl Gottfried:** Conceptualization, Methodology, Writing - review & editing. **Christopher Gundler:** Conceptualization, Funding acquisition, Writing - review & editing. **Sylvia Nürnberg:** Conceptualization, Supervision, Writing - review & editing. **Claudia Langebrake:** Conceptualization, Funding acquisition, Supervision, Writing - review & editing. **Adrin Dadkhah:** Conceptualization, Data curation, Formal analysis, Funding acquisition, Investigation, Methodology, Project administration, Resources, Software, Visualization, Writing - original draft, Writing - review & editing.

Declaration of Competing Interest

The authors declare that they have no known competing financial interests or personal relationships that could have appeared to influence the work reported in this paper.

Figure Captions

Figure 11: 3D printed PLA sinker, scale in cm

Figure 12: Pictures of DPE printed tablets, scale in cm; a): small and large cylinder of P20/34-M, P25/29-M, P30/24-M and P25/29-CSM. b): Donuts and Oblongs of P25/29-M

Figure 13: DPE printhead, modified with force feeder

Figure 14: DSC diagrams of the APIs (only first heating cycle); top - LD, bottom – CD

Figure 15: TGA thermogram of the APIs

Figure 16: DSC Diagrams of the excipients (only first heating cycle), powder blend and filament; top to bottom: Kollicoat[®] IR, Kollidon[®] VA64, Mannitol, powder blend, filament

Figure 17: Isothermal (182 °C) section of DSC runs (exotherm up); top - CD, bottom - powder blend

Figure 18: Isothermal (180 °C) TGA thermogram of CD

Figure 19: Dissolution diagram (LD) of the six different tablets of formulation P25/29-M (n = 6)

Figure 20: Dissolution diagram (CD) of the six different tablet of formulation P25/29-M (n = 6)

Graphical abstract

Development of 3D printed Levodopa / Carbidopa tablets to be used in a hospital's digital Closed Loop Medication Management

